Resistive transition anisotropy in superconducting granular ceramics: Interplay of effective medium approximation and percolation

L. Burlachkov,[1] E. Mogilko,[2] Y. Schlesinger,[2] Y. M. Strelniker,[3] and S. Havlin[3]

[1]*Institute of Superconductivity and Department of Physics, Bar-Ilan University, Ramat-Gan 52900, Israel*

[2]*Department of Physics, Bar-Ilan University, Ramat-Gan 52900, Israel*

[3]*Minerva Center, Jack and Pearl Resnick Institute of Advanced Technology*
and Department of Physics, Bar-Ilan University, Ramat-Gan 52900, Israel

The resistive transition $\rho(T,H)$ in granular high-T_c superconductors is described by a combination of the effective-medium approximation for anisotropic mixtures with the percolation theory. We found a single parameter accounting for both the structural anisotropy as well as for the intrinsic resistivity anisotropy of a single grain. We obtained a direct (no fitting parameters) estimate of the superconducting volume fraction f as a function of temperature, as well as of the percolation threshold f_p and of the zero-resistivity threshold f_0. The model describes successfully the experimental $\rho(T,H)$ dependence at different relative directions of the c axis, the current j and the magnetic field H in $Bi_2Sr_2CaCu_2O_{8-x}$ ceramics. We provided estimates for the value of the Josephson critical current between grains. The latter proves to be strongly suppressed even by weak magnetic fields $H < 750$ Oe. This results in the appearance of the field-induced excess resistivity $\Delta\rho$ that obeys the dependence $1/\Delta\rho \simeq 1 + H_\phi/H$, where H_ϕ is the characteristic field trapped by a single Josephson contact.

PACS number(s): 74.81.Bd, 74.72.Hs, 74.50.+r

I. INTRODUCTION

The nature of the resistive transition $\rho(H,T)$ and its relation to the percolation phenomena in high-T_c superconducting granular ceramics remain an intriguing subject of intensive investigations for more than 15 years.[1–5] The problem is of great importance not only for a better understanding of the transport and magnetic properties of these compounds, but also for their applications as superconducting devices, such as cables, magnets, etc. The granular structure of the high-T_c ceramics is exhibited by a dispersion of the intrinsic transition temperature T_c among different grains. Therefore within the transition region, such a ceramic is a mixture of superconducting and normal grains (SN mixture). The problem one faces is to describe consistently its transport and magnetic properties starting from T_{onset}, which corresponds to the appearance of the first superconducting grain [or the first deviation of $\rho(T)$ from its normal behavior], down to T_0 where the resistivity drops to zero. The latter temperature is determined by the percolation of the superconducting currents throughout the sample. The transition region can be quite wide, e.g., $T_{onset} - T_0 \gtrsim 10$ K in typical $Bi_2Sr_2CaCu_2O_{8-x}$ ceramics. This results not only from a variation of local T_c but also from dispersion of the orientation of grains[6] with respect to the external magnetic field H, from a nonhomogeneous distribution of fields and currents in the sample, etc. The challenging problems are determining the superconducting volume fraction $f(T)$, the Josephson critical current between grains $I_w(T)$ (here w stands for weak), and other characteristics of the high-T_c ceramics, from the experimental $\rho(H,T)$ data.

Thus far, several models were introduced in order to describe the percolation of transport current through the network of Josephson contacts between superconducting grains, such as "brick-wall"[7] and "rail-switch"[8] models (see also

an interesting numerical comparison[9] of these models). Both models appear to be quite useful for the description of critical current in Bi-based ceramics and tapes. However, in terms of the resistive transition, these models deal explicitly with the low-temperature part of the $\rho(T)$ curve, where all (or almost all) of the grains are already superconducting, the resistivity is much less than the normal one and is determined exclusively by the Josephson contacts between grains.

In this paper we suggest an approach that accounts for the interplay between percolation of superconducting currents through the weak links and spreading of the resistive transition due to dispersion of the critical temperature (variation of T_c among different grains). The latter is usually described by the effective-medium approximation (EMA),[10] which proves to be very useful for the description of SN mixtures.[11–15] However, EMA by itself is incapable of analyzing the whole resistive transition $\rho(T)$, especially its low-temperature part, where T approaches T_0. We combine the EMA, generalized for anisotropic mixtures,[14,16,17] with the theory of percolation of transport currents in SN mixtures.[18–21] These two theories prove to be mutually complementary and together provide an effective tool for the analysis of the resistive transition region in high-T_c ceramics.

The critical current in our approach is determined phenomenologically (by the density of channels in the percolating spanning cluster). Thus we are not "competing" with the brick-wall[7] or rail-switch[8] models whose goal is to describe in detail the structure of percolating superconducting currents in the low-temperature part of the $\rho(T)$ curve. Instead, we analyze the resistivity in the whole temperature region starting from T_{onset} down to T_0.

Using our method we find $f(T)$ directly, without any fitting parameters involved. We emphasize the difference between the percolation threshold $f_p \equiv f(T_p)$ that manifests to the appearance of a superconducting spanning cluster while
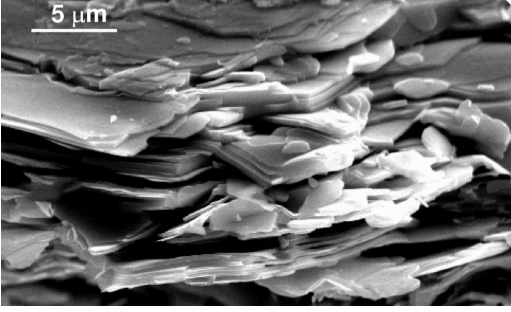
FIG. 1. The transmission electron microscope image of $Bi_2Sr_2CaCu_2O_{8-x}$ ceramics plateletlike morphology.

$\rho(T_p)$ remains finite, and the zero-resistivity threshold $f_0 \equiv f(T_0) \geqslant f_p$ that corresponds to $\rho = 0$. This difference results from the fact that at $f = f_p$ the spanning cluster is infinitely "thin" and cannot carry any finite transport current I. We find that for $Bi_2Sr_2CaCu_2O_{8-x}$ (BSCCO) ceramics one can neglect the difference between f_p and f_0 only for extremely small currents $I \lesssim 1$ μA that can hardly be achieved in experiments. We show that the EMA provides a good description of the resistive transition at $f < f_p$, i.e., at $T_{onset} > T > T_p$. At $f_p < f < f_0$ (i.e., $T_p > T > T_0$) the sample should be considered as consisting of the spanning cluster and the nonspanning part connected in parallel. A combination of the EMA and the percolation theory helps to describe the $\rho(T)$ data in this region and to estimate the Josephson critical currents I_w between grains. We also analyze the effect of the magnetic field on the transition and prove that small magnetic fields $H < 0.1$ T affect the system mainly by suppressing I_w.

We determine a single parameter q that characterizes the effective anisotropy for $T > T_p$. The latter accounts for both the structural anisotropy of BSCCO (large aspect ratio of platelet-shaped grains) and the anisotropy of the normal resistivity of a single grain. For typical BSCCO ceramics these two sources of anisotropy largely compensate each other, thus the resulting effective anisotropy proves to be quite modest.

II. EXPERIMENT: RESULTS AND DISCUSSION

Pellets of $Bi_2Sr_2CaCu_2O_{8-x}$ (Ref. 22) were uniaxially compacted at room temperature under the pressure of 310 MPa, and then sintered at 860 °C for 100 h. The x-ray spectra show the presence of an essentially single-phase $Bi_2Sr_2CaCu_2O_{8-x}$, exhibiting about 87% alignment of the platelet grains, with the c axis parallel to the direction of the compaction. The electron microscope image, see Fig. 1, shows that the grains are of a plateletlike shape, with an average lateral length-to-thickness aspect ratio $m = r_{ab}/r_c \approx 100$. Here $r_{ab} \simeq 10$ μm and $r_c \simeq 0.1$ μm are the characteristic semiaxes of the grains in the ab plane and along the c axis, respectively, if the grains are considered as oblate spheroids. The sample was cut into a parallelepiped of dimensions $2.3 \times 5.8 \times 1.9$ mm^3, the latter size is along the c axis. Six gold contacts were applied to the sample by sputtering. The resistivity was measured by the standard four-probe
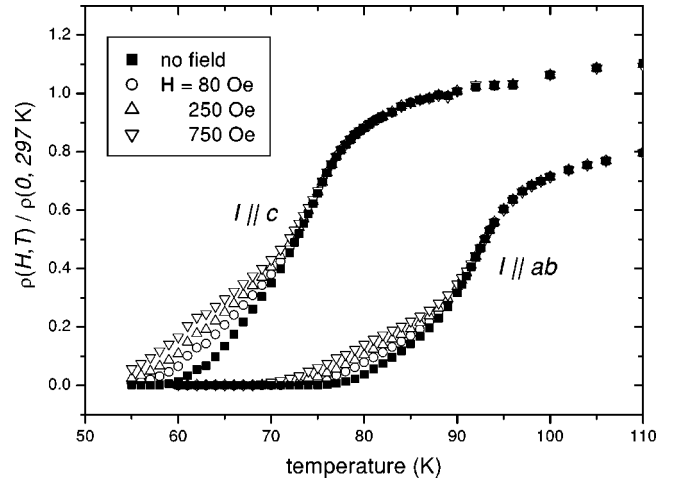

FIG. 2. Experimentally obtained resistivities for $I \| ab$ (ρ_{ab}) and for $I \| c (\rho_c)$, normalized by the room-temperature resistivity. One can notice that ρ_{ab} is almost independent of magnetic field at $T > T_H^{ab} \approx 92$ K, and the same applies to ρ_c at $T > T_H^c \approx 75$ K.

method as a function of temperature and weak magnetic fields $H \leqslant 750$ Oe, and then analyzed using the magnetic-field excess resistance method.[23] The measurements were carried out with the current direction both perpendicular and parallel to the c axis. The changes in the relative orientations of the current, the field, and the c axis of the sample were performed by a corresponding choice of current and voltage contacts. Thus the sample position in the cryostat was kept fixed during the whole set of measurements, ensuring a constant thermal contact. We refer to the resistivities obtained with I perpendicular to the c axis (i.e., in the ab plane) and parallel to it as ρ_{ab} and ρ_c, respectively. The total current was $I = 100$ mA for both directions, corresponding to current densities $j_{ab} = 1$ A/cm^2 and $j_c = 0.75$ A/cm^2. The magnetic field effect was examined for H parallel and perpendicular to the current for both current directions, so the measurements were carried out in four different configurations: $H \perp (I \| ab)$, $H \| I \| ab$ for ρ_{ab} and $H \| I \| c$, $H \perp (I \| c)$ for ρ_c.

In Fig. 2 we show the results for two configurations: $H \perp (I \| ab)$ and $H \perp (I \| c)$. The temperature T_{onset} that corresponds to the beginning of the transition appears to be different in the two cases: $T_{onset}^{ab} \approx 100$ K for $I \| ab$ and $T_{onset}^c \approx 85-90$ K for $I \| c$. One obtains an even more drastic difference for zero-resistance temperature: $T_0^{ab} \approx 75$ K and $T_0^c \approx 57$ K if determined by the condition $\rho(T_0)/\rho(T_{onset}) \simeq 10^{-3}$ at $H = 0$.

The results for the other two configurations indicate that the direction of the magnetic field is practically unimportant. In Fig. 3 we compare the field-induced excess resistivity $\Delta \rho_{ab}(H,T) = [\rho_{ab}(H,T) - \rho_{ab}(H=0,T)]$ normalized by $\rho_{ab}^n(T)$ for $H \perp I$ and $H \| I$. Here $\rho_{ab}^n(T)$ is the extrapolation of the linear (normal) part of the $\rho_{ab}(T)$ curve from $T > 100$ K down to low temperatures. We see that $\Delta \rho_{ab}$ shows weak dependence on the field direction. Such an effect has already been reported[1] in high-T_c ceramics at low magnetic fields $H < 0.1$ T. This rules out the dissipative motion of vortices as a source for the appearance of the excess resistivity. Otherwise at $H \perp I$ one should obtain a much greater $\Delta \rho$ than
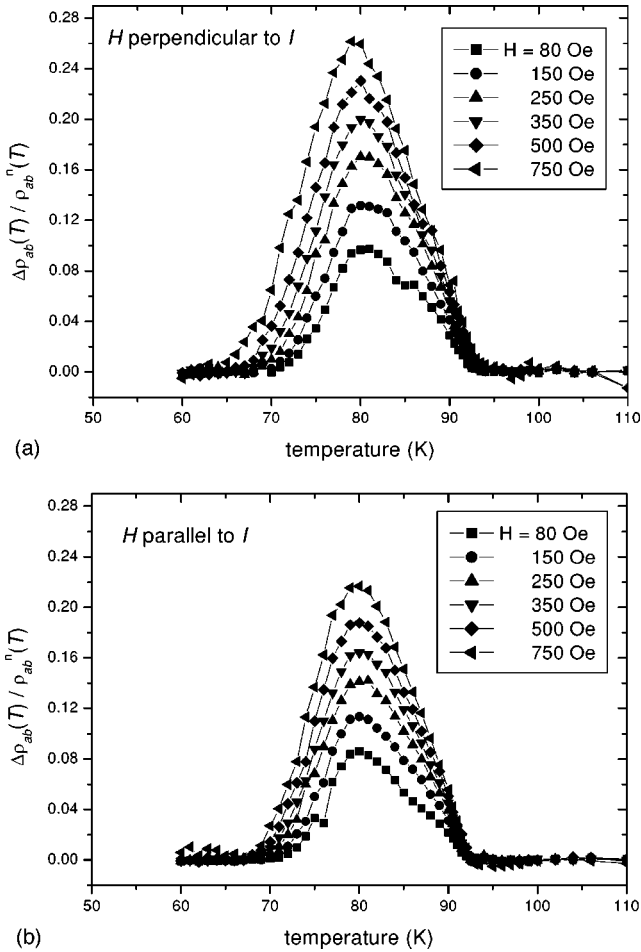
FIG. 3. Excess resistivity $\Delta\rho_{ab}(H,T)=\rho_{ab}(H,T)-\rho_{ab}(0,T)$ [divided by the normal resistivity $\rho^n(T)$] induced by small magnetic fields $H\leq750$ T at (a) $H\perp I$, (b) $H\|I$.

at $H\|I$, since in the latter case the Lorentz force appears only owing to the field and current bending inside the sample. Moreover, the measured values $\Delta\rho(H)\simeq0.20$–0.25 are too large when compared to the Bardeen-Stephen result[24] for unpinned vortices: $\Delta\rho(H)/\rho^n\approx H/H_{c2}\lesssim10^{-2}$ in our low-field range $H\leq750$ Oe. Similar results hold for $\Delta\rho_c$. Therefore we expect that the field dependence of the resistivity for low H results solely from the suppression of the weak links (Josephson contacts) between the superconducting grains.[25] The weak link mechanism is also supported by the fact that the upper parts of $\rho_{ab}(T)$ and $\rho_c(T)$ for $T>T_H^{ab}\approx92$ K and $T>T_H^c\approx75$ K, respectively, are almost field independent. For these high temperatures the share of the Josephson currents in corresponding directions is negligibly small (since $f<1$ and most grains are still normal, $I_w(T)$ is weak, etc.), and the resistivity $\rho(T)$ depends exclusively on $f(T)$. The latter, as we see below, cannot be changed by weak magnetic fields $H<0.1$ T. The presence of the field-independent part in the resistive curves $\rho(T)$ provides a direct proof for the importance of accounting for the superconducting volume fraction $f(T)$ and rules out the picture where all the grains undergo a superconducting transition at T_{onset}, and the further decrease of ρ is determined by the dependence of the Josephson criti-

cal currents on temperature. For such a scenario both $\rho_{ab}(T)$ and $\rho_c(T)$ should significantly depend on H starting from T_{onset}, and one should expect a sudden drop of both resistivities at T_{onset}, which has not been observed.

III. ANALYSIS

A. Effective-medium approximation

The $Bi_2Sr_2CaCu_2O_y$ ceramics are strongly anisotropic due to two reasons. First, the normal resistivity of grains (single crystals) is highly anisotropic: $\rho_c^n/\rho_{ab}^n\simeq10^4$ (Refs. 26–28) at $T=50$–100 K. Second, there is a large structural anisotropy due to the platelet shape of grains. In our sample the typical aspect ratio m of the grains is about 100, see Fig. 1. Thus the anisotropic, self-consistent version of EMA (Refs. 14,16 and 17) that accounts for both sources of anisotropy should be applied. Since the misorientation of grains in our sample is small, see Fig. 1, the c axes of all the grains are assumed to be mutually parallel. The resistivity of the normal grains is characterized by a two-component resistivity tensor, $\rho_{ab}^n(T)$ and $\rho_c^n(T)$, whereas for superconducting grains, naturally, $\rho=0$. The volume fractions of superconducting and normal grains are $f(T)$ and $1-f(T)$, respectively. Strictly speaking, f depends on the magnetic field as well. However, for low fields $H\leq750$ Oe used in our experiment, the shift of the transition temperature, $\Delta T_c(H)\approx H(dH_{c2}/dT)^{-1}$, is negligibly small. Thus one can consider f to be practically field independent.

The effective resistivities of such a mixture, $\rho_{ab}^{eff}(T)$ and $\rho_c^{eff}(T)$, are determined by the EMA equations:[14]

$$\tilde{\rho}_c=\frac{L-f}{L}, \quad \tilde{\rho}_{ab}=\frac{1-L-2f}{1-L}, \tag{1}$$

where $\tilde{\rho}_c=\rho_c^{eff}/\rho_c^n$ and $\tilde{\rho}_{ab}=\rho_{ab}^{eff}/\rho_{ab}^n$ are the normalized effective resistivities, the depolarization function $L(q\tilde{\rho}_{ab}/\tilde{\rho}_c)$ is defined as

$$L(x)=\frac{x}{2(1-x)^{3/2}}\left\{\ln\left(\frac{1+\sqrt{1-x}}{1-\sqrt{1-x}}\right)-2\sqrt{1-x}\right\}$$

$$\text{for} \quad x<1, \tag{2}$$

$$L(1)=\frac{1}{3}, \tag{3}$$

$$L(x)=\frac{x}{x-1}\left\{1-\frac{1}{\sqrt{x-1}}\tan^{-1}(\sqrt{x-1})\right\} \quad \text{for} \quad x>1, \tag{4}$$

and $q=m^2\rho_{ab}^n/\rho_c^n$. Note that since L depends on $\tilde{\rho}_c$ and $\tilde{\rho}_{ab}$, Eqs. (1) form a self-consistency problem and should be solved numerically. However, certain properties of the solution can be found analytically, namely, (i) the solution depends on a single parameter q that accounts for both structural (m) and resistive (ρ_{ab}^n/ρ_c^n) anisotropies; (ii) $\tilde{\rho}_c(f)$ and $\tilde{\rho}_{ab}(f)$ vanish simultaneously at $f_p=1/3$ at any q, i.e., the
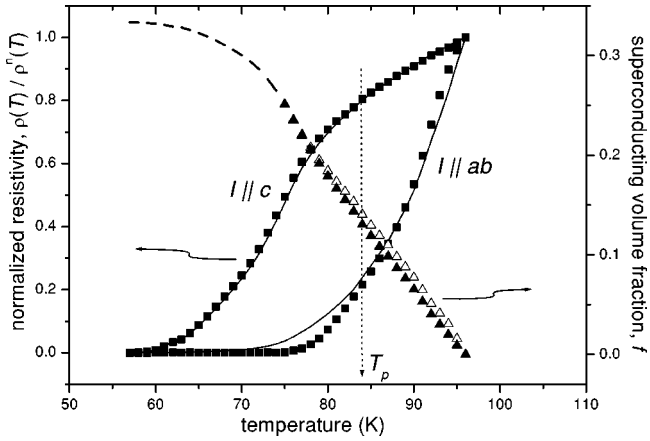
FIG. 4. Squares represent the normalized resistivities $\tilde{\rho}$ $= \rho(T)/\rho^n(T)$ (denoted in the text as $\tilde{\rho}_{ab}$ for $I \| ab$ and as $\tilde{\rho}_c$ for $I \| c$) at $H=0$. Triangles show the calculated superconducting volume fraction f as a function of temperature. Solid triangles are obtained with Eq. (5) and the open ones are obtained with a reduced expression $f \approx (1-\tilde{\rho}_c)/(3-2\tilde{\rho}_c)$, see discussion in the text. The procedure of determination of f is justified at $T > T_0^{ab} \approx 75$ K. The nonphysical values obtained for f at $T < T_0^{ab}$ are indicated with a dashed line. The dotted line indicates the percolation temperature T_p, which corresponds to the percolation threshold $f_p \approx 0.17$.

percolation threshold found for isotropic EMA holds for its anisotropic generalization as well; (iii) for $q>1$ we get $\tilde{\rho}_c(f) > \tilde{\rho}_{ab}(f)$ and vice versa; (iv) at $q=1$ we get the well-known EMA result[12] $\tilde{\rho}_{ab} = \tilde{\rho}_c = 1 - 3f$; and (v) the superconducting volume fraction f can expressed via $\tilde{\rho}_{ab}$ and $\tilde{\rho}_c$ as

$$f = \frac{1 - \tilde{\rho}_c - \tilde{\rho}_{ab}(1-\tilde{\rho}_c)}{3 - \tilde{\rho}_{ab} - 2\tilde{\rho}_c}. \tag{5}$$

In our case $\tilde{\rho}_{ab}(T)$ and $\tilde{\rho}_c(T)$ are obtained experimentally, whereas $f(T)$ and q are to be determined. It is important that f is independent of q, see Eq. (5), and, therefore, can be determined from the experimental data directly, without any fitting procedure. The effective anisotropy q includes two factors: $m^2 \simeq 10^4$ and $\rho_{ab}^n/\rho_c^n \simeq 10^{-4}$. They largely compensate each other, and thus both cases $q>1$ and $q<1$ are, in principle, possible. In our case $q>1$ since we experimentally get $\tilde{\rho}_c > \tilde{\rho}_{ab}$ for all temperatures.

In Fig. 4 we show $\tilde{\rho}_{ab}$ and $\tilde{\rho}_c$ as functions of T at $H=0$ and analyze these data in the following way. First, using Eq. (5), we find the superconducting volume fraction f as a function of T that is also shown in Fig. 4 by solid triangles. Note that since $\tilde{\rho}_{ab} \ll \tilde{\rho}_c$ for all temperatures except the very onset of the transition, one can neglect $\tilde{\rho}_{ab}$ in Eq. (5) and get f $\approx (1-\tilde{\rho}_c)/(3-2\tilde{\rho}_c)$, see open triangles in Fig. 4. This means that in our case $f(T)$ is determined mainly by $\tilde{\rho}_c$. After replotting $\tilde{\rho}_{ab}$ and $\tilde{\rho}_c$ as functions of f instead of T, see Fig. 5(a), we solve Eqs. (1) and find the anisotropy parameter q that provides the best fit for the $\tilde{\rho}(f)$ curves. It appears that the upper (low-f, or high-T) part of the resistive transition
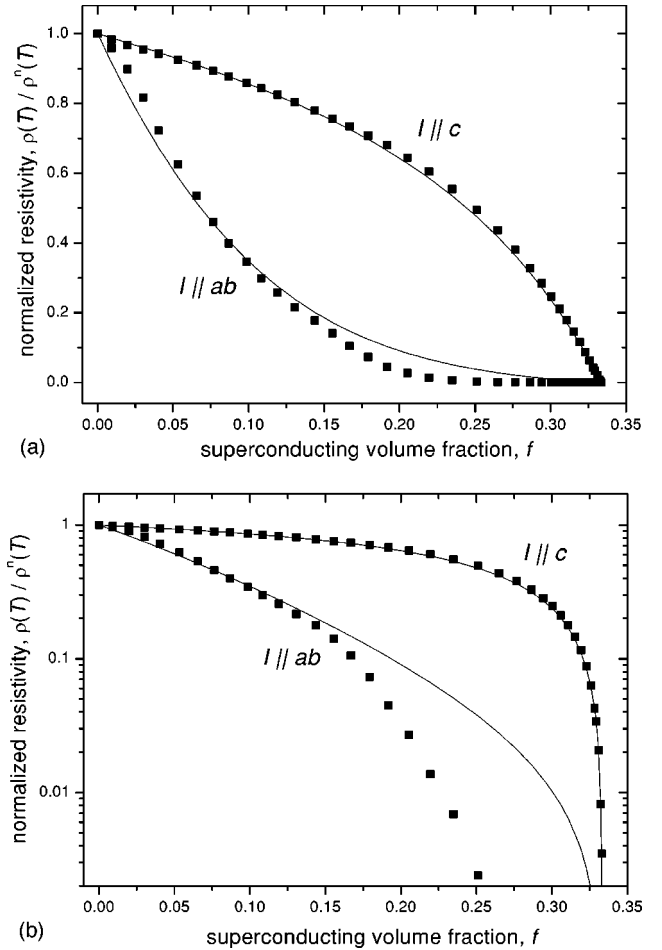

FIG. 5. Normalized resistivities $\tilde{\rho}_{ab}$ and $\tilde{\rho}_c$ (squares) at $H=0$ plotted in (a) linear and (b) logarithmic scales as functions of the superconducting volume fraction f. The lines represent the EMA fit obtained by numerical solution of Eqs. (1) at $q=36$.

can be adequately described by Eqs. (1), with the best fit achieved at $q=36$ if only the data points with $f<0.17$ are considered. At larger $f \gtrsim 0.17$, as we see from Fig. 5(a), and especially from Fig. 5(b) where the logarithmic scale for the resistivity data is applied, $\tilde{\rho}_{ab}$ starts to drop much faster and cannot be approximated with the solution of Eqs. (1) at any q. For $\tilde{\rho}_c$ the fit is almost perfect for the whole temperature range. Note that due to mutual compensation of m^2 and ρ_{ab}^n/ρ_c^n, the effective anisotropy $q=36$ is much less than one might intuitively expect for such highly flattened grains.

In order to understand the above results better, we show in Fig. 6 the results of the numerical solution of Eqs. (1) for different $q \gtrsim 1$. One can notice that for large $q \gtrsim 10$, which our optimal $q=36$ belongs to, the resistivity $\tilde{\rho}_c(f)$ becomes almost saturated and close to the limiting case $q \to \infty$. At the same time $\tilde{\rho}_{ab}(f)$ strongly depends on q and (for $q \gtrsim 10$) is much less than $\tilde{\rho}_c(f)$, except at the very beginning of the transition, where $f \ll 1$. This result has a clear physical meaning that can be easily understood if we consider the situation where $\rho_{ab}^n = \rho_c^n$ and, correspondingly, the effective anisotropy q is equal to m^2. In such a case, embedding a superconduct-
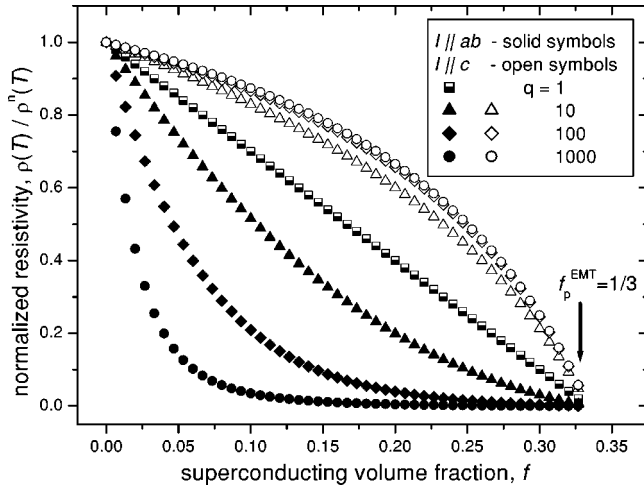
FIG. 6. Numerical solution of Eqs. (1) for $\tilde{\rho}_{ab}$ and $\tilde{\rho}_c$ (solid and open symbols, respectively) at various $q \geqslant 1$. The half-solid squares correspond to $q=1$ (no anisotropy), where the two resistivities coincide. Both $\tilde{\rho}_{ab}$ and $\tilde{\rho}_c$ vanish at $f=f_p^{EMT}=1/3$.

ing oblate spheroid with $m \gg 1$ into the normal isotropic matrix does not affect significantly the current and the equipotential lines for $I \| c$, see Fig. 7(a). As a result, at $f \ll 1$ the resistivity is almost unchanged: $\tilde{\rho}_c \approx 1$ and further increasing of m has almost no effect on $\tilde{\rho}_c$ at any f. Quite the contrary, for $I \perp c$ both current and equipotential lines are strongly affected by such an embedded spheroid, see Fig. 7(b). Therefore $\tilde{\rho}_{ab}$ drops significantly already at $f \ll 1$ and further elongation of the superconducting spheroid parallel to j results in additional decrease in $\tilde{\rho}_{ab}$.

It is clear from Figs. 5 and 6 that the apparent difference between T_{onset}^{ab} and T_{onset}^c, mentioned when discussing Figs. 2 and 4, is just an artifact. The beginning of the transition is better determined at $I \| ab$, since even small f causes a sharp drop of $\tilde{\rho}_{ab}$. Thus the real T_{onset} is equal to $T_{onset}^{ab} \approx 96-98$ K as has been reported for many similar $Bi_2Sr_2CaCu_2O_{8-x}$ ceramics.[3,29] For $I \| c$ and $q \gtrsim 10$ the resistivity $\tilde{\rho}_c$ drops very slowly at small f, therefore the onset of the transition, if determined by the $\rho_c(T)$ data, becomes smeared out and apparently shifts towards the low temperatures.

The perfect fit obtained for $\tilde{\rho}_c(T)$ at all temperatures, see Fig. 4, should not be considered as an evidence for the ability of EMA to consistently describe the experimental data. Its quality results from the combination of two already mentioned reasons: (i) practical independence of $f(T)$ on $\tilde{\rho}_{ab}$ and (ii) weak dependence of $\tilde{\rho}_c(T)$ on q for $q \gtrsim 10$. Therefore, the true test of the applicability of EMA in our case is its ability to fit $\tilde{\rho}_{ab}(T)$. We see from Figs. 4 and 5 that this fit is quite reasonable for $f < 0.17$ but fails at larger f, where $\tilde{\rho}_{ab}$ drops much faster than predicted by EMA. Another apparent inconsistency is the presence of two different zero-resistivity temperatures: $T_0^{ab} \approx 75$ K and $T_0^c \approx 57$ K, as if there exist two different percolation thresholds for $I \| ab$ and $I \| c$, whereas EMA predicts $f_p = 1/3$ for both current directions. Moreover,
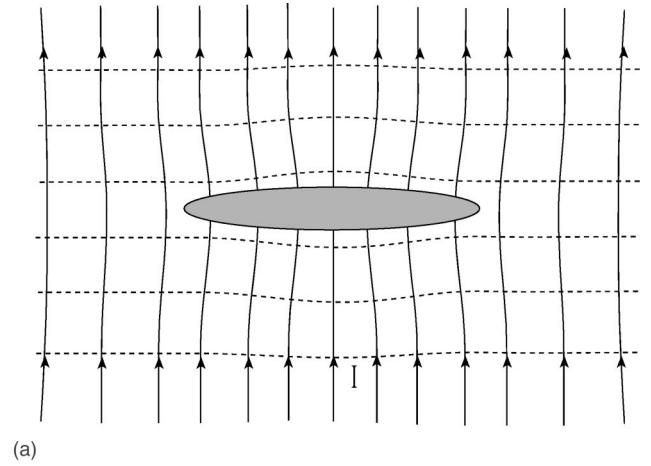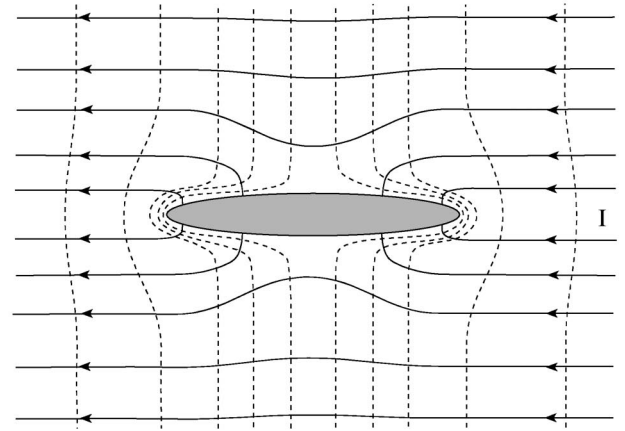
FIG. 7. Oblate superconducting ellipsoid with isotropic resistivity embedded into a normal matrix where its short axis c is (a) parallel, (b) perpendicular to the current. In the case (a) the current and equipotential lines remain mostly unaffected, and the resistivity does not change much. In the case (b) the effect on the current and equipotential lines is great and, correspondingly, there is a significant reduction of resistivity.

one needs also to explain the noticeable dependence of the resistivities on the magnetic field H, which looks surprising since f is almost independent of H for the low fields used in our experiments.

B. Percolation of the superconducting currents

To resolve the seeming contradictions mentioned just above, one should combine the EMA and the percolation theory. The latter has been successfully used for the description of the transport current in high-T_c ceramics.[2,5,6,30,31] Below we show that the EMA and the percolation theory are mutually complementary, and their combination consistently describes the experimental $\rho(H,T)$ in the whole temperature range of the superconducting transition.

In the SN mixtures one should clearly discriminate between the "zero-resistance" concentration $f_0 = f(T_0)$ determined by the condition $\rho(T_0) = 0$, and the percolation threshold f_p that manifests the first appearance of the span-

ning superconducting cluster. The latter consists of percolating channels.[18] Let n be their density in the direction of the current. Each channel can carry the Josephson critical current I_w without destroying superconductivity in the weak links between grains. Of course, I_w depends on the current direction and on temperature. The spatial variation of I_w in a similar ceramic ($Bi_{1.8}Pb_{0.4}Sr_2Ca_2Cu_3O_{8+x}$) was studied in Ref. 30, where the direct dependence of I_w on the grain alignment and dispersion of the grain sizes was found. The high quality of the grain alignment in our sample and reasonable uniformity of the grains assure that the spatial variation of I_w (at given temperature and direction of current) is not great. We find another proof for relative constancy of I_w below when analyzing the effect of the magnetic field on the resistive transition $\rho(T)$.

The maximal superconducting current that the spanning cluster can withstand is $I_{span}=j_{span}S$, where $j_{span}=nI_w$ and S is the cross section of the sample. Zero resistance is achieved at $f=f_0\equiv f(T_0)$ where the spanning cluster carriers the total transport current: $I_{span}(T_0)=I$. Obviously, f_0 is a function of I and $f_0(I)\gtrsim f_p$, where the equality is reached at very weak transport currents $I\sim I_w$. The latter condition can be hardly realized experimentally since $I_w\simeq0.1-10\ \mu A$, as we show below. The critical behavior of resistivity, $\rho\propto(f_p-f)^\mu$, obtained using the percolation theory,[18–20] is valid only in the same limit $I\rightarrow I_w$, $f_0\rightarrow f_p$. We demonstrate below that in most experimental cases, including the present one, the current I is large enough to cause a significant difference between f_0 and f_p.

Let us find both f_p and f_0 for our sample. As we discussed above, the EMA, including its anisotropic generalization, provides $f_p^{EMA}=1/3$. However, the EMA is not the right tool for obtaining the percolation thresholds, and this value exceeds significantly the exact results obtained using the percolation theory (see Refs. 18–21 as reviews) for the continuum media, $f_p^{cont}\approx0.17$ or for dense lattices, $f_p^{latt}\approx0.20$. Recent experiments[5] show that the $Bi_2Sr_2CaCu_2O_{8-x}$-$BiFeO_3$ composites ($BiFeO_3$ is an insulator) undergo percolation transition at low temperatures, where all the $Bi_2Sr_2CaCu_2O_{8-x}$ grains are superconducting, provided their volume fraction is greater than 20%. This confirms that for such mixtures $f_p<0.2$. For the grains that belong to the spanning cluster, the basic EMA procedure of balancing the excess currents (see, for instance, Refs. 11 and 20) no longer holds since I_{span} does not depend on the normal resistivity of nonsuperconducting grains. Therefore it is not surprising that EMA fails to fit the $\widetilde{\rho}_{ab}$ data at $f>f_p$. As we obtained in the preceding section, the EMA fails to fit the data at $f>0.17$, so it is reasonable to accept $f_p=f_p^{cont}\approx0.17$ for our sample. Since $f_p=f(T_p)$, we get $T_p\approx80$ K.

At $f>f_p\approx0.17$ the SN mixture consists of the spanning superconducting cluster and the nonspanning part, connected in parallel. The spanning cluster has zero voltage if it carries a current that does not exceed I_{span}. At higher currents the weak links become normal and the voltage rises instantly. The nonspanning part has a smooth I-V characteristic. Therefore we can assume that the spanning cluster carries a current that slightly exceeds I_{span} in order to keep the volt-

ages in the two parallel resistors equal. Correspondingly, the nonspanning part carries slightly less than $I-I_{span}$. In order to find I_{span}, let us notice that n grows proportionally to η^{-2}, where $\eta\propto(f-f_p)^{-\nu}$ is the correlation length of the percolation problem and $\nu\approx0.9$.[18] Thus we get

$$n_{ab}=\gamma(f-f_p)^{2\nu}/s_{ab}\quad(I\|ab),\qquad(6)$$

$$n_c=\gamma(f-f_p)^{2\nu}/s_c\quad(I\|c),\qquad(7)$$

where $\gamma\simeq1$ is a numerical coefficient and s is the cross section of a grain perpendicular to the current, i.e., $s_{ab}=\pi r_{ab}r_c$ and $s_c=\pi r_{ab}^2$. Note that $n_{ab}/n_c=r_{ab}/r_c=m\approx100$. Zero resistance is achieved, as we discussed, at $j=j_{span}=nI_w$. Using this condition and Eqs. (6) and (7), we find two similar equations:

$$[f(T_0^{ab})-f_p]^{2\nu}\approx\frac{I_g^{ab}}{I_w^{ab}(T_0^{ab})},\qquad[f(T_0^c)-f_p]^{2\nu}\approx\frac{I_g^c}{I_w^c(T_0^c)}$$
$$(8)$$

for the determination of T_0^{ab} and T_0^c, and, in turn, $f_0^{ab}=f(T_0^{ab})$ and $f_0^c=f(T_0^c)$. Here $I_g=js$ is the mean transport current that crosses a single grain, and s stands for either s_{ab} or s_c depending on the current direction. Note that j is constant in our experiment, therefore $I_g^c/I_g^{ab}=m\simeq100$.

C. Interplay between the EMA and the percolation theory

Now we can construct a consistent description of all the experimental data using both the EMA and the percolation theory. For $f<f_p\approx0.17$, which corresponds to $T>T_p\approx80$ K, the spanning cluster is absent and the EMA provides a good fit for the experimental data, see Figs. 4 and 5. At lower temperatures, $T<T_p$, i.e., at $f>f_p$, the ceramics is divided into the spanning cluster and the rest of the media. The spanning cluster carries $I_{span}\approx SnI_w$, whereas the nonspanning part carries $I-I_{span}$. The Josephson critical current is proportional to either the tunnel conductivity[32] or the depairing current,[24] depending on the weak link type. In any case, for BSCCO one should expect that I_w^{ab} and I_w^c are quite different, namely, $I_w^{ab}\gg I_w^c$. In other words, the Josephson currents in the ab plane are "strong" weak links, whereas those in c direction are "weak" weak links. A similar picture has been considered in Refs. 33 and 34. Since $n_{ab}/n_c=m\approx100$, we undoubtedly get $I_{span}^{ab}\gg I_{span}^c$ at the same temperature. Therefore, for $I\|c$ the condition $I_{span}^c\ll I$ holds well above f_p, and $\widetilde{\rho}_c$ remains almost unaffected by the appearance of the spanning cluster. As we discussed in the preceding section, $f(T)$ is determined mainly by $\widetilde{\rho}_c(T)$. Thus we can use the EMA procedure to determine $f(T)$ even below T_p. The EMA fails to describe $\widetilde{\rho}_{ab}(T)$ there, but the latter has negligible effect on $f(T)$, see the minor difference between the solid and open triangles in Fig. 4. We see also from Fig. 4 that f depends on temperature almost linearly at $T>70$ K. This means that the T_c distribution function, $c(T)\propto df/dT$, appears to be almost constant in this temperature range. At $T<70$ K the EMA apparently fails for direct determination of $f(T)$ because I_{span}^c becomes of the order of

I, and the condition $I_{span}^c = I$ is fulfilled around $T = T_0^c \approx 57$ K. Linear extrapolation of $f(T)$ provides $f_0^c \approx 0.48$, and from Eq. (8) one finds $I_w^c(57\ \text{K}) \approx 15\ \mu\text{A}$ which looks reasonable.

Quite the contrary, the appearance of the spanning cluster at $f_p \approx 0.17$ affects $\tilde{\rho}_{ab}$ almost immediately, since I_{span}^{ab} becomes of the order of I just above f_p. Thus $\tilde{\rho}_{ab}$ drops at $f > f_p$ much faster than predicted by EMA and vanishes at $T_0^{ab} \approx 75$ K which corresponds to $f_0^{ab} \approx 0.25$. From Eq. (8) we get $I_w^{ab}(T = T_0^{ab} \approx 75\ \text{K}) \approx 3\ \mu\text{A}$.

D. The effect of the magnetic field

Above we analyzed the experimental results obtained in the absence of magnetic field. However, even weak fields $H \lesssim 750$ Oe affect the resistive transition quite appreciably, see Figs. 2 and 3. This looks surprising since the influence of such weak fields on $f(T)$ is negligible, as we discussed above. One should expect a considerable decrease of f only in high fields $H > 5$ T, see Ref. 6 and references therein.

The excess resistivity induced by the magnetic field, $\Delta\rho$, appears to be almost independent of the direction of the field with respect to the grains and even with respect to the current, see Fig. 3. As mentioned above, this confirms that the field affects the pointlike weak links and that the resistivity associated with the vortex motion is negligible in our case.

In the presence of magnetic field the resistive curves $\rho(T)$ split below a certain temperature T_H that can be estimated from Figs. 2 and 3 as $T_H^{ab} \approx 92$ K for $I\|ab$ and $T_H^c \approx 75$ K for $I\|c$. Above T_H the resistivity is almost field independent. This can be understood easily if we notice that the Josephson critical current I_w vanishes as T approaches T_{onset}, whereas I_g does not depend on temperature, so just below T_{onset} we have $I_w \ll I_g$. In this situation the magnetic field that further suppresses I_w has almost no effect on ρ. The latter becomes "field sensitive" provided $I_w \simeq I_g$. Correspondingly, the condition that determines T_H is

$$I_w^{ab}(T_H^{ab}) \simeq I_g^{ab}, \qquad I_w^c(T_H^c) \simeq I_g^c. \qquad (9)$$

Since $I_g^c/I_g^{ab} = m \approx 100$, it is clear that T_H^c should be considerably less than T_H^{ab}, as observed experimentally. Moreover, Eq. (9) provides another tool for the estimation of I_w, and we readily obtain $I_w^{ab}(92\ \text{K}) \approx 0.03\ \mu\text{A}$, $I_w^c(75\ \text{K}) \approx 2\ \mu\text{A}$. The fact that $T_H^{ab} > T_p$, i.e., the effect of the magnetic field on ρ_{ab} becomes noticeable even in the absence of the spanning cluster, does not contradict our approach. Suppression of I_w results in the appearance of additional resistivity in the nonspanning part also, but the quantitative analysis of this effect is rather difficult, requiring numerical simulations and will be carried out elsewhere.

It is worth mentioning that the presence of well-defined splitting points T_H^{ab} and T_H^c, determined by Eq. (9), confirms our assumption on relative spatial uniformity of I_w in both directions. Moreover, independence of ρ on H at $T > T_H$ justifies the fact that it is impossible to describe the $\rho(T)$ curve considering solely the Josephson contact network without
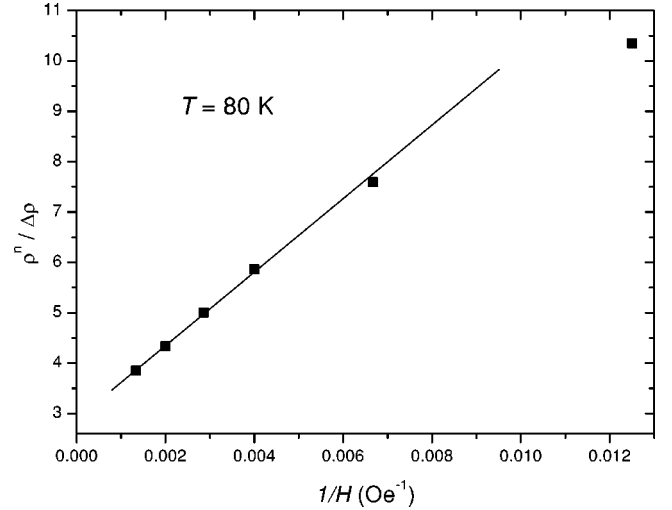

FIG. 8. Inverse excess resistivity (see Fig. 3) normalized by the normal one, $\rho^n/\Delta\rho$, plotted as a function of inverse magnetic field $1/H$ at $T = 80$ K. The straight line is a guide for the eye.

introducing the superconducting volume fraction $f(T)$. In other words, the percolation theory does not provide a consistent picture without EMA.

The particular dependence of $\Delta\rho$ on H can be found as follows. After crude averaging the well-known Fraunhofer-like expression $I_w(H) = I_w^0 |\sin(\pi H/H_\phi)|/(\pi H/H_\phi)$ (for instance, see in Ref. 24) over the areas and directions of the weak links, one gets an oversimplified interpolation formula

$$I_w(H) \simeq I_w^0 H_\phi /(\pi H + H_\phi). \qquad (10)$$

Here I_w^0 is the value of the critical Josephson current in the absence of field, $H_\phi = \phi_0/s_w$, ϕ_0 is the unit flux, and s_w is the mean area of the Josephson contact. We omit the indices ab and c since the analysis is similar for both directions of current. When the field is switched on, a current $\Delta I = I_w^0 - I_w(H) = I_w^0 \pi H/(\pi H + H_\phi)$ is expelled from a superconducting grain and flows through the normal matrix. This leads to the increase of the normal current density j_n by $\Delta j = n_w \Delta I$, where n_w is the density of weak links in the sample cross section perpendicular to the current. Note the difference between n_w and n_{span}: the latter counts only for the weak links that belong to the spanning cluster, so always $n_w \geqslant n_{span}$. Moreover, n_w is finite even at $f < f_p$ (where $n_{span} = 0$), therefore the effect of the magnetic field on resistivity can be noticeable even for $T > T_p$. The superconducting current density j_s is decreased by the same amount, thus $j_s + j_n$ remains constant and equal to the total current density j. The additional heat dissipation owing to the magnetic field is $\Delta Q = (j_n + \Delta j)^2 \rho^n - j_n^2 \rho^n \simeq 2 j_n \Delta j \rho^n$. On the other hand, $\Delta Q = j^2 \Delta\rho$, where $\Delta\rho$ is the increase of the measured (effective) resistivity. Thus we immediately get

$$\frac{\rho^n}{\Delta\rho} \simeq \frac{j^2}{2 j_n N_w I_w^0} \left(1 + \frac{H_\phi}{\pi H} \right). \qquad (11)$$

In Fig. 8 we plot $\rho^n/\Delta\rho_{ab}$ as a function of $1/H$. At $H > 150$ Oe we get an almost perfect straight line in accor-
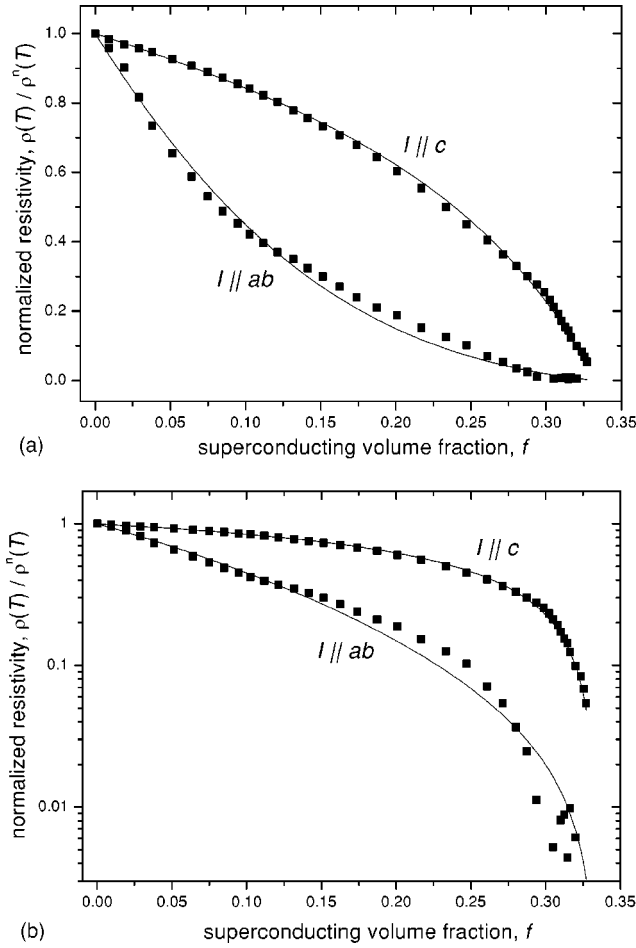
FIG. 9. The same as Fig. 5 but at $H=750$ T and $q=17$. The EMA fit works better for this case (compare with Fig. 5), especially for $f>f_p\approx0.17$. See discussion in the text.

dance with Eq. (11). Only the $H=80$ Oe point deviates from this line, probably because of the inaccuracy of the interpolation formula Eq. (10) at $H\lesssim H_\phi$. It is worth noting that Eq. (11) predicts a saturation of $\Delta\rho$ at high fields, with $(\Delta\rho)_{max}\simeq 2j_n N_w I_w^0 \rho^n/j^2\simeq 2N_w I_w^0 \rho^n/j$, since at high fields j_s is highly suppressed and $j_n\approx j$. The linear extrapolation of our experimental data shown in Fig. 8 towards $1/H=0$ provides $(\Delta\rho)_{max}=0.36\rho^n$. Note also that $N_w I_w^0$ is the Josephson critical current density, so Eq. (11) describes its saturation at high fields.[35]

Finally, in Fig. 9(a) we show the results of the EMA fit for the $\rho(T)$ data at $H=750$ Oe, i.e., at the maximal magnetic field we used in our experiment, where the weak links are highly suppressed by the field: $I_w<I_g$. We see that in this case EMA describes both branches $\rho_{ab}(T)$ and $\rho_c(T)$ quite consistently, and even the logarithmic scale, see Fig. 9(b), does not reveal significant deviations of $\rho_{ab}(T)$ from its EMA fit at low temperatures [compare with Fig. 5(b) that corresponds to $H=0$]. On the other hand, EMA should provide a better fit when the weak links are "open," i.e., at $I_w>I_g$, and one might expect the best results from the EMA at $H=0$. The explanation is quite simple. There are two obstacles for the applicability of the EMA in superconducting

ceramics. First, the presence of finite I_w results in additional resistivity not accounted for by EMA. Second, the percolation of current via the spanning cluster breaks the consistency of the EMA and requires consideration of the two-resistor model. As magnetic field grows on, we get two competing effects: appearance of the additional resistivity due to suppression of weak links that should worsen the EMA fit, and suppression of I_{span} which works in favor of the applicability of the EMA. The latter effect proves to be decisive, since the spanning cluster is responsible for the very fast drop of ρ_{ab} at $T<T_p$ in the absence of the field. Therefore it is not surprising that at $H=750$ Oe we get a consistent EMA picture at all $T>T_H^c\approx75$ K, whereas at $H=0$ the applicability of the EMA is restricted by the condition $T>T_p\approx80$ K.

IV. SUMMARY

We have developed a method of analysis for the resistivity data $\rho(H,T)$ in high-T_c ceramics, such as BSCCO, YBCO, and similar compounds, with well-oriented grains (c axes are almost parallel). Our analysis is based on mutual complementarity of the effective-medium approximation (EMA), generalized for anisotropic media, and of the percolation theory, generalized in order to account for the presence of weak links between the grains. To implement this method, one needs to know the resistivity data in both directions: ρ_{ab} and ρ_c. We analyzed the data obtained in $Bi_2Sr_2CaCu_2O_{8-x}$ and found the superconducting volume fraction $f(T)$ and the parameter of the effective anisotropy q that accounts for both the platelet shape of the grains (aspect ratio $m\approx100$) and for the anisotropy of the normal resistance of a single grain ($\rho_c^n/\rho_{ab}^n\simeq10^4$). These two sources of anisotropy partially compensate each other, so the resulting q can be quite moderate. We obtained in our case $q\approx36$.

The applicability of the EMA depends on f. At high temperatures, where $f<f_p\approx0.17$, the EMA describes perfectly both ρ_{ab} and ρ_c. At $f>f_p$ the spanning cluster appears, and the ceramics should be considered as consisting of two parallel resistors: the spanning cluster and the nonspanning part. The current in the spanning cluster is determined by the carrying capacity of the weak links (Josephson junctions) between grains, and zero resistivity is achieved only at $f_0>f_p$ when the spanning cluster is "thick" enough to carry the whole transport current I flowing in the sample without destroying the superconductivity in the weak links. Also, f_0 is a function of the current direction. The difference between f_p and f_0 depends on I and vanishes as $I\to I_w$. However, this can hardly be achieved in experiments, and even at low current densities $j\simeq1$ A/cm^2 used in our experiment the difference between f_p and f_0 (and, correspondingly, between T_p and T_0) proves to be quite significant. Our analysis enables an estimation of the critical Josephson current I_w in both directions: in the ab plane and along the c axis.

Even a weak magnetic field $H<0.1$ T suffices to considerably suppress I_w, resulting in a noticeable increase of re-

sistivity $\Delta\rho$. We analyzed the dependence of $\Delta\rho$ on H and found that it can be described adequately by our two-resistor model. We explained the presence of characteristic temperatures T_H^{ab} and T_H^c, above which the resistivity is not sensitive to the magnetic field. The values of T_H provide another estimation for I_w.

This method should be useful for the analysis of the basic properties of the superconducting ceramics, as well as for their technological applications.

[1] Y. Iye, S. Nakamura, T. Tamegai, T. Terashima, and Y. Bando, Proceedings of MRS '89 Fall Meeting, Boston, 1989 (unpublished).

[2] E. Babić *et al.*, Phys. Rev. B **45**, 913 (1992); M. Prester, E. Babić, M. Stubičar, and P. Nozar, *ibid.* **49**, 6967 (1994); M. Prester and Ž. Marohnić, *ibid.* **51**, 12 861 (1995).

[3] V. Garnier, R. Calliard, A. Sotelo, and G. Desgardin, Physica C **319**, 197 (1999).

[4] H. Enomoto, N. Mori, I. Matsubara, and H. Ozaki, Physica B **284–288**, 579 (2000).

[5] H. Nadifi, A. Ouali, C. Grigorescu, H. Faqir, O. Monnereau, L. Torlet, G. Vacquier, and C. Boulesteix, Supercond. Sci. Technol. **13**, 1174 (2000).

[6] L.I. Glazman, A.E. Koshelev, and A.G. Lebed', Sov. Phys. JETP **67**, 1235 (1988).

[7] L.N. Bulaevskii, J.R. Clem, L.I. Glazman, and A.P. Malozemoff, Phys. Rev. B **45**, 2545 (1992).

[8] B. Hensel, J.-C. Grivel, A. Jeremie, A. Perin, A. Pollini, and R. Flükiger, Physica C **205**, 329 (1993); B. Hensel, G. Grasso, and R. Flükiger, Phys. Rev. B **51**, 15 456 (1995).

[9] B. Zeimetz, R.P. Baranowski, and J.E. Evetts, J. Appl. Phys. **88**, 5283 (2000).

[10] R. Juretschke, R. Landauer, and J.A. Swanson, J. Appl. Phys. **27**, 838 (1956); D.A.G. Bruggeman, Ann. Phys. (Leipzig) **24**, 636 (1935).

[11] A. Davidson and M. Tinkham, Phys. Rev. B **13**, 3261 (1976).

[12] T.C. Choy and A.M. Stoneham, J. Phys.: Condens. Matter **2**, 939 (1990).

[13] A.L. Korzhenevskii and A.A. Luzhkov, Physica C **204**, 191 (1992).

[14] Z.D. Genchev, Supercond. Sci. Technol. **6**, 532 (1993).

[15] D.V. Shantsev, M.E. Gaevski, R.A. Suris, A.V. Bobyl, V.E. Gasumyants, and O.L. Shalaev, Phys. Rev. B **60**, 12 485 (1999).

[16] D. Stroud, Phys. Rev. B **12**, 3368 (1975).

[17] D.J. Bergman and Y.M. Strelniker, Phys. Rev. B **60**, 13 016 (1999).

[18] B. I. Shklovski and A. L. Efros, *Electronic Properties of Doped Semiconductors*, (Springer, New York, 1984).

[19] A. Coniglio, in *Physics of Finely Divided Matter*, edited by N. Boccara and M. Daoud (Springer, New York, 1985).

[20] J.P. Clerc, G. Giraud, J.M. Laugier, and J.M. Luck, Adv. Phys. **39**, 191 (1990).

[21] *Fractals and Disordered Systems*, edited by A. Bunde and S. Havlin (Springer-Verlag, Berlin, 1996).

[22] The high-temperature superconducting powder was purchased from the Single Crystal Institute, Kharkov, Ukraine.

[23] Y. Schlesinger, L. Burlachkov, and E. Mogilko, Physica C **307**, 291 (1998).

[24] M. Tinkham, *Introduction to Superconductivity* (McGraw-Hill, New York, 1996).

[25] J. Paasi, P. Kottman, M. Majoroš, and V. Plecháček, Physica C **305**, 21 (1998).

[26] W. Jihong, C. Genghua, Chu Xi, Y. Yifeng, Z. Dongning, M. Zhenhong, Y. Qiansheng, and Z. Zhongxlan, Supercond. Sci. Technol. **1**, 27 (1988).

[27] S. Martin, A.T. Fiory, R.M. Fleming, G.P. Espinosa, and A.S. Cooper, Appl. Phys. Lett. **54**, 72 (1989).

[28] M.P. Maley, J.H. Cho, S. Fleshler, and L.N. Bulaevskii, Appl. Supercond. **2**, 667 (1994).

[29] S. Nomura, H. Yoshino, and K. Ando, Physica C **196**, 323 (1992).

[30] A.E. Pashitski, A. Polyanskii, A. Gurevich, J.A. Parrell, and D.C. Larbalestier, Physica C **246**, 133 (1995).

[31] A. Gurevich, Phys. Rev. B **42**, 4857 (1990).

[32] V. Ambegaokar and A. Baratoff, Phys. Rev. Lett. **10**, 486 (1963); **11**, 104(E) (1963).

[33] M. Dhallé, M. Cuthbert, M.D. Johnston, J. Everett, R. Flükiger, S.X. Dou, W. Goldacker, T. Beales, and A.D. Caplin, Supercond. Sci. Technol. **10**, 21 (1997).

[34] B. Hensel, G. Grasso, and R. Flükiger, Phys. Rev. B **51**, 15 456 (1995).

[35] K. Sato, T. Hikata, H. Mukai, M. Ueyama, N. Shibita, T. Kato, T. Masuba, M. Nagata, K. Iwata, and T. Mitsui, IEEE Trans. Magn. **27**, 1231 (1991).